Both the He ion implantation and Fe ion irradiation actually inhibit each other's radiation damage to the material. This may play a positive role in reducing radiation damage to the $Ti_3AlC_2$ material, and also provides new insight into irradiation resistance of this material.

## 5 - 5 Helium Irradiation Induced Microstructural Damages and Mechanical Response of $Al_2O_3$-$ZrO_2$-SiC Composites*

Zhu Yabin, Chai Jianlong, Niu Lijuan, Shen Tielong and Wang Zhiguang

Numerous helium atoms would be produced in nuclear structural materials due to the (n, α) nuclear transmutation reaction. As a potential structural material, the $Al_2O_3$-$ZrO_2$-SiC composite was irradiated with 2.0 MeV He-ions and its structure and mechanical response were investigated.

X-ray diffraction analyzation gives that there are small shifts and broadening of the diffraction peaks, which denotes lattice expansion resulted from residual tensile stress related to the formation of defects and helium bubbles upon irradiation. TEM observations show that He bubbles with nanometer size can be observed in all irradiated regions for all samples, even in the near-surface regions where the expected He concentration is rather low (Fig. 1). The large number of grain/phase boundaries related to the refined grains is responsible for the formation of bubbles in the near-surface region which would accelerate the migration of implanted He-ions, as the mobility of He atoms at the boundary is higher than that within the grains. Moreover, the distribution of He bubbles in the $Al_2O_3$, $ZrO_2$ and SiC grains was obviously different: most of bubbles are uniformly distributed in $Al_2O_3$ grains and partly distributed

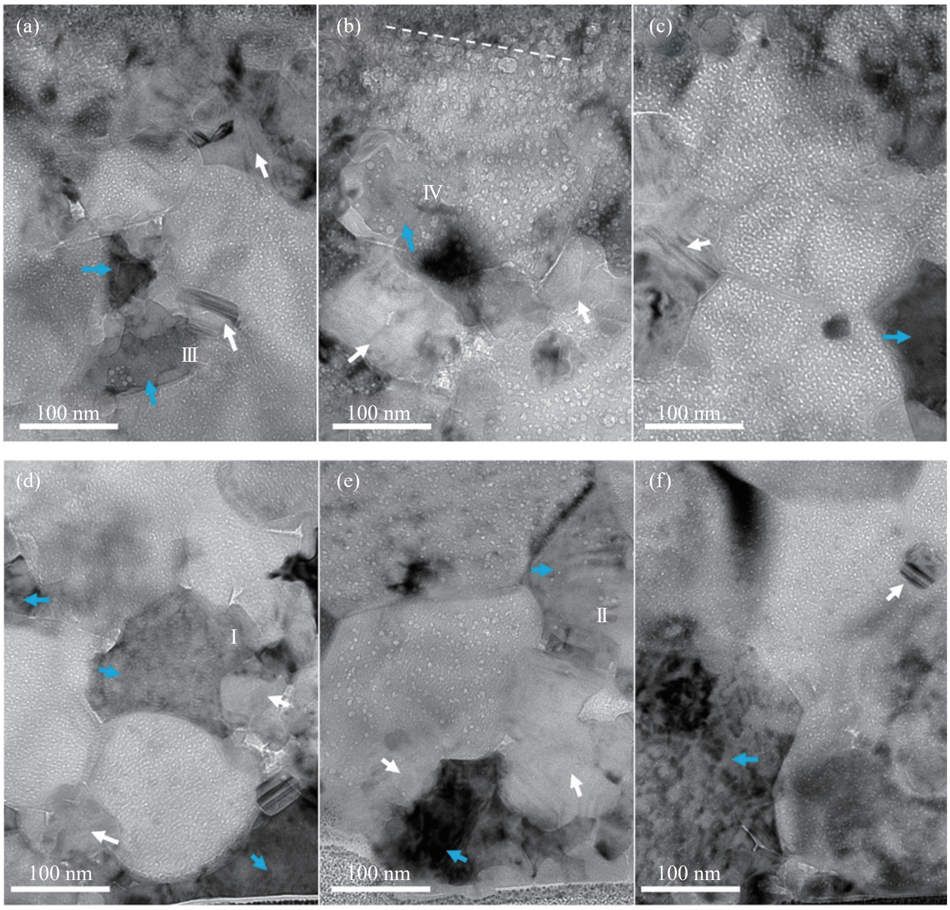


Fig. 1 (color online) Bright field under-focused (bubbles are with white contrast) TEM micrographs obtained from the He concentration peak regions of 800 ℃-$1.72\times10^{17}$ (a), 800 ℃-$1.72\times10^{18}$ (b), 300 ℃-$1.72\times10^{18}$ (c) and the near-surface regions of 800 ℃-$1.72\times10^{17}$ (d), 800 ℃-$1.72\times10^{18}$ (e), 300 ℃-$1.72\times10^{18}$ (f). The $ZrO_2$ and SiC grains are indicated by the light blue and white arrows. The dash line in (b) highlights a continuous band of large, interconnected bubbles at the He concentration peak region.

in $ZrO_2$ grains while no detectable bubbles are observed in SiC grains. The uniformly distributed bubbles in $Al_2O_3$ grains (even close to the grain boundaries) imply the bubbles are stable under the irradiation conditions in present work. Unlike the $Al_2O_3$ grains, the implanted He ions inside the $ZrO_2$ grains first agglomerated into small bubbles with high density (region I in Fig. 1(d)) and then grew and coalesced to large bubbles with a reduced number density (region II in Fig. 1(a), region III in Fig. 1(e) and region IV in Fig.1(b)) at higher He concentration. This indicates that there is a critical number density of small He bubbles in $ZrO_2$ grains. Above this critical number density, the bubbles will interact with each other to form large ones. No bubbles inside the SiC grains with size of 50∼200 nm were observed due to the high migration.

Figure 2 shows the average micro-hardness and elastic modulus varying with indentation depth of the pristine and irradiated samples. As observed, the microhardness remains almost unchanged for the 800 ℃-1.72×$10^{17}$ sample, and a slight reduction was observed for the 800 ℃-1.72×$10^{18}$ sample, while there is a slight irradiation induced hardening for the 300 ℃-1.72×$10^{18}$ sample. The detailed values and relative changes of micro-hardness and elastic modulus in the range of 50∼300 nm were obtained, which gives that the discrepancies of micro-hardness and elastic modulus between pristine and irradiated samples were found to be minor with approximately 4%. The bubble formation results in the softening of the sample irradiated at 800 ℃, while the irradiation induced point defects is the main factor for the hardening of the sample irradiated at 300 ℃. The elastic modulus, which is related to bond density and stiffness (interatomic potential energy), is reduced after irradiation when the incident ions damage the crystal structures of composites.

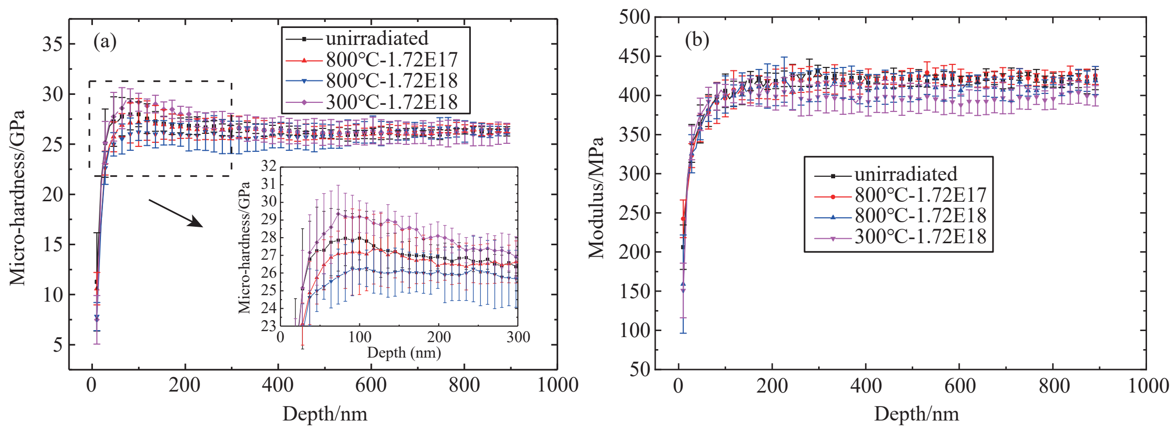


Fig. 2 (color online) Micro-hardness (a) and elastic modulus (b) as a function of indentation depth of the pristine and irradiated composites.

The absence of micro-cracks and peeling as well as the barely changed hardness and elastic modulus implies that $Al_2O_3$-$ZrO_2$-SiC composite are promising as irradiation-tolerant materials.

* Foundation item: National Key R&D Program of China (2022YFB3708500) and National Natural Science Foundation of China (12205349)